AIP | Applied Physics Letters

Adiabatic fiber microtaper with incorporated an air-gap microcavity fiber Fabry-Pérot interferometer

Cheng-Ling Lee, Ching-Yi Tai, Chien-Lin Chen, and Pin Han

Citation: Applied Physics Letters **103**, 033515 (2013); doi: 10.1063/1.4815994
View online: http://dx.doi.org/10.1063/1.4815994
View Table of Contents: http://scitation.aip.org/content/aip/journal/apl/103/3?ver=pdfcov
Published by the AIP Publishing

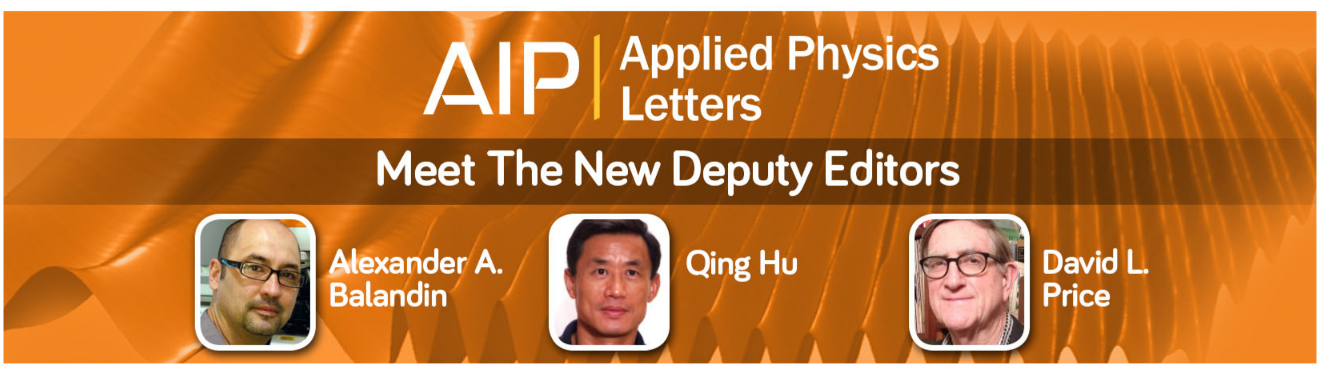

APPLIED PHYSICS LETTERS 103, 033515 (2013)

Adiabatic fiber microtaper with incorporated an air-gap microcavity fiber Fabry-Pérot interferometer

Cheng-Ling Lee,[1,a)] Ching-Yi Tai,[1,2] Chien-Lin Chen,[1] and Pin Han[2]
[1]Department of Electro-Optical Engineering, National United University, Miaoli 360, Taiwan
[2]Graduate Institute of Precision Engineering, National Chung Hsing University, Taichung 402, Taiwan

(Received 21 May 2013; accepted 1 July 2013; published online 18 July 2013)

This study demonstrates an adiabatic fiber microtaper with incorporated an air-gap microcavity fiber-Fabry-Pérot-interferometer to perform superior sensing characteristics. Optical interference fringes with good fringes contrast within bandwidth of 1250–1650 nm are performed experimentally. A highly spectral sensitivity of peak power with +3.65 dB/°C (+9759 dB/RIU) is achieved when the device is operated under a fundamental-mode-cutoff (FMC) condition. By measuring peak power of the fringe, one can determine the temperature (T) or refractive index of environment. The proposed hybrid sensor is further applied to measure high T (∼1000 °C) of surrounding in non-FMC condition that obtains a good linearity of spectral response. © *2013 AIP Publishing LLC*. [http://dx.doi.org/10.1063/1.4815994]

Adiabatic fiber microtapers (AFMTs) have been reported in many powerful applications such as fiber couplers,[1] high sensitive sensors,[2–5] optical microfiber resonators,[6] and supercontinuum generation.[7] The adiabatic fiber taper is drawing very smoothly by the heat-pulling with a flame to make the fiber diameter changing very slowly. The artificial rearrangement of the new fiber waveguide structure enables single mode fiber (SMF) to have some modified and distinctive modal characteristics. An SMF with pure silica cladding diameter of 125 μm tapering into few tens of micrometers, the tapered waist almost plays as a new core since the remained original core is almost dissolved. The optical mode field expands over the fiber waist after micro-tapering, thus the effective index (propagation constant) of the fundamental-mode will be changed. The evanescent wave in the taper stretch out or not is strongly dependent with the surrounding refractive index (RI). Thus, the optical characteristics of the fiber taper can be strongly changed by the external medium. Therefore, since the coupling mechanism of the well known long-period fiber grating (LPFG) is based on the fundamental core mode coupling to the cladding modes so that is sensitive to the external parameters. Thus many studies about the fiber microtapers incorporated with the LPFGs have been proposed.[3,4] However, the above LPFGs fabricated on the fiber microtapers do have some difficulties and complicated processes since the taper would be very easy to break when it is further processed by the vacuum coating[3] and femto-second laser writing.[4] For the reasons, it seems not very effective and practical.

In this study, we propose an AFMT merged with an air-gap microcavity fiber Fabry-Pérot interferometer (FFPI) for sensitively measuring the temperature or refractive index of the environment. Respecting the FFPIs are very useful and sensitive in the many applications,[8–11] there were some fiber devices that incorporated with the FFPIs for some sensing purposes have been presented. These works have demonstrated the incorporation of the fiber sensors can achieve the multiple sensing capabilities and new functionalities.[10,11] For the above reasons, we can estimate the new configuration proposed in this paper, the integration of the AFMT and air-gap microcavity FFPI can achieve the new and sensitive characteristics since the adiabatic fiber microtaper is used, as shown in Fig. 1. Experimental results demonstrate that superior sensing characteristics are performed for sensing temperature (T) or refractive index (RI) when the sensor operated under a condition of fundamental mode cutoff (FMC) in the AFMT. In addition, the proposed all-fiber sensor also can be used as a high T sensor (up to 1000 °C) which is of functional flexibility of the measurements and much attractive in the practical applications.

The developed hybrid device was first fabricated by very slowly tapering single mode fiber (SMF-28) into a structure with diameter of around several tens of micrometers (μm) and taper length of about several centimeters. Figure 2 shows the experimental setup for the heat pulling to make the adiabatic microtapers. The SMF was pulled by force and heated with a flame of hot zone temperature of around 1100 °C. Fabrication parameters with tapering time and pulling force are respectively 25 min and 2 g weight to

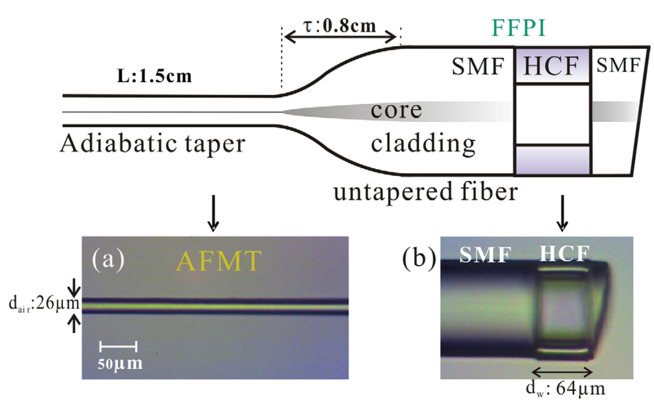

FIG. 1. Schematic diagram of the proposed hybrid fiber sensor. Insets show the micrographs of the used AFMT and air-gap microcavity FFPI, respectively. Here, AFMT: adiabatic fiber microtaper, SMF: single mode fiber, HCF: hollow core fiber.

[a)]Email: cherry@nuu.edu.tw

achieve the adiabatic taper with the given structure. Optical response of the developed taper is promptly measured by an optical spectrum analyzer (OSA) with use of a broadband light source (BLS) in a wavelength range of $1250 \sim 1650$ nm launched. The tapering processes would cause the corresponding remaining core to be almost vanished and enable the dopant germanium (Ge) in the core to diffuse out into pure-silica cladding.[12] After the fiber was tapered, it was further fabricated by cleaving one side of the non-taper and splicing an AGMFFPI fabricated by the sandwiched structure of SMF-HCF(hollow core fiber)-SMF to make an in-line air-gap microcavity FFPI incorporated, as shown in Fig. 1. Figure 1 shows the diagram of the proposed hybrid fiber device and insets (a) and (b), respectively, display the microphotographs of the AFMT and air-gap microcavity FFPI fiber tip. Here, L is uniform taper length, τ is taper transition length, and d_w the taper waist. In the fabrication of the proposed FFPI, only the method of the fusion splicing is used, but the device end should be further cleaved the SMF end into a non-flat surface with a tilt angle to avoid the undesired Fresnel reflection of the SMF/Air endface, as shown in the inset (b) of the Fig. 1. The transmission spectra of the fabricated AFMT are shown in Fig. 3(a). Inset shows the structure of the used microtaper with taper length $L = 1.5$ cm, transition length $\tau = 0.8$ cm, and taper waist of $d_w = 26\,\mu$m with under FMC. The FMC condition is occurred when the effective index of fundamental-mode of the fiber taper approaches to (almost equals) the refractive index of the surrounding. However, the details of the principle about the FMC based on an index-matching liquid surrounding around the taper have been discussed in the published work.[2]

In general, the fundamental-mode is confined well in the tens-micrometers tapered fiber with air surrounding and propagates along the taper which is approximately adiabatic and just like propagating in a non-tapered single mode fiber (SMF-28). The spectrum has no cut off wavelength and high transmission (<1 dB average loss), as shown in the brown line (in air) of the Fig. 2(a). However, a special case with FMC occurs when the tapered microfiber was in an index-matching at one wavelength (i.e., cutoff wavelength: λ_c). The Cargille® optical liquid that is suitable for yielding the FMC is used to fill the entire length of the sensor. The condition can produce a sharp increase in spectral loss of the fundamental mode at λ_c that exceeds the FMC, the effective index of the fundamental mode is lower than that of surrounding to achieve a non-guiding leakage situation. The power of the leakage mode dissipates out of the taper and

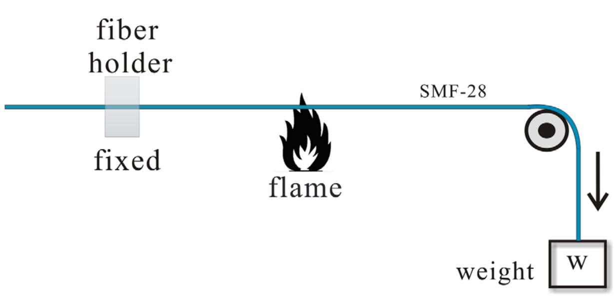

FIG. 2. Experimental setup of the heat pulling for fabricating the adiabatic micro-tapers.

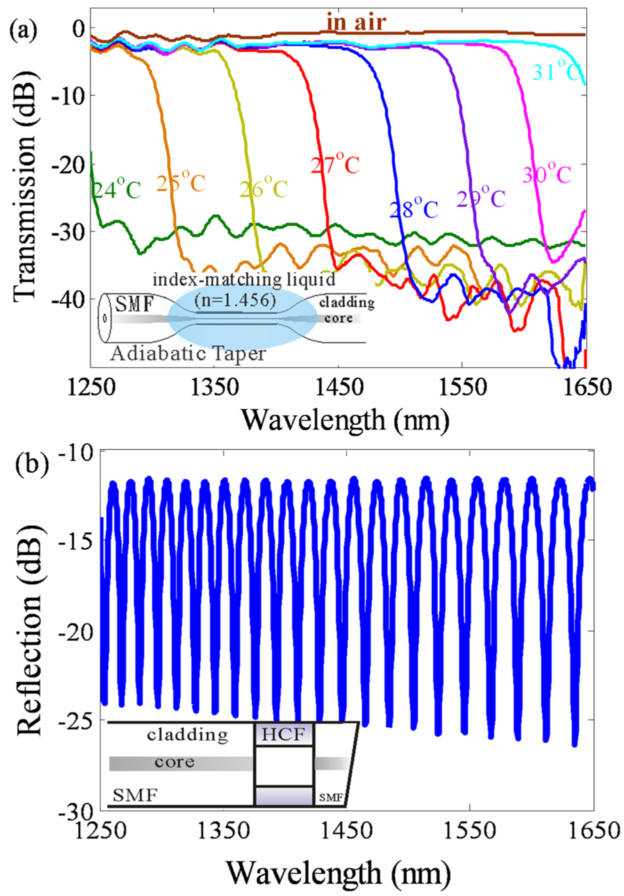

FIG. 3. (a) Transmission spectra of the used AFMT with taper waist $d_w = 26\,\mu$m in the non-FMC (in air) and FMC conditions (index-matched). (b) Reflection spectrum of the used FFPI with air gap $d_{air} = 64\,\mu$m. Insets of (a) and (b), respectively, show the corresponding structure to the optical spectra.

not guides in the fiber anymore to perform a high loss in long wavelength region which is demonstrated and plotted in the Fig. 3(a). The use of the index-matched optical liquid as the surrounding performs a short-pass edge filter performance and the λ_c greatly shifts to the longer wavelength side when the T increases. The optical characteristics present the FMC phenomena of the proposed tapered fiber are extremely sensitive to the surrounding T in the FMC conditions. However, the short-pass cutoff profile strongly depends on the taper quality and tapered structure. It is difficult to monitor a spectral peak or wavelength dip variation to estimate the change of the spectral response once the surrounding parameters varies. When we combined an assisted all-fiber device with simple and high visibility spectra, e.g. FFPI, as shown in Fig. 3(b), the new optical properties can be expected and amazed. The Fig. 3(b) shows the reflection spectrum of the used FFPI with air gap $d_{air} = 64\,\mu$m and good visibility of over 0.93 is achieved. The nice visibility is ascribed to the good parallel of the Fabry-Pérot cavity (two SMF/HCF interfaces) since cavities with tilt angles would degrade the interference performance of the FFPI.[13]

Figure 4(a) illustrates that in the non-FMC condition of the incorporated hybrid device (shown in the Fig. 1), the light from the microtaper inputs the proposed FFPI connected in the microtaper end, it respectively reflects by the SMF/air and air/SMF interfaces of the FFPI and obtains an

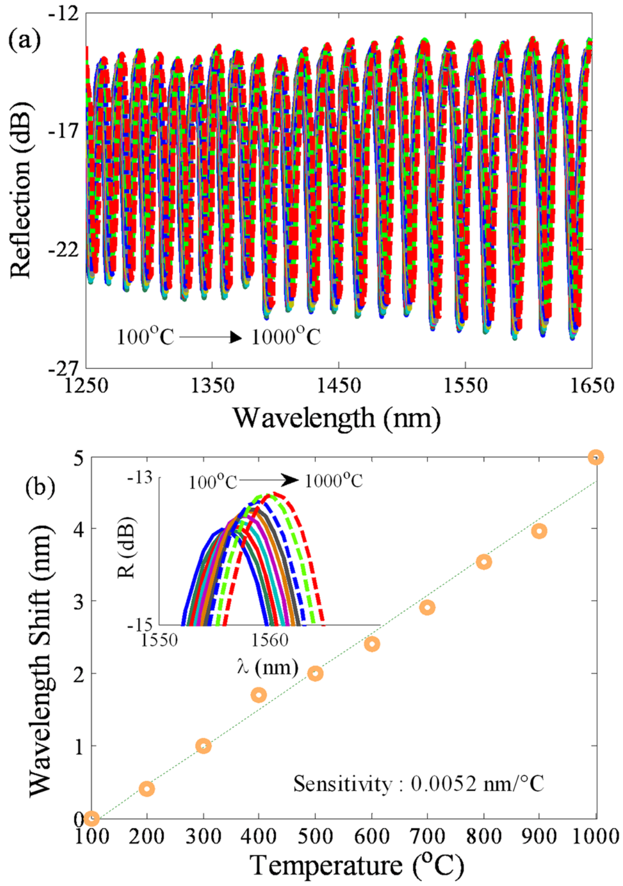

FIG. 4. (a) Experimental spectra of the interference peak shifts ($\Delta\lambda$) of the proposed hybrid fiber sensor under the non-FMC condition for high T sensing and (b) the T sensitivity of $\Delta\lambda$.

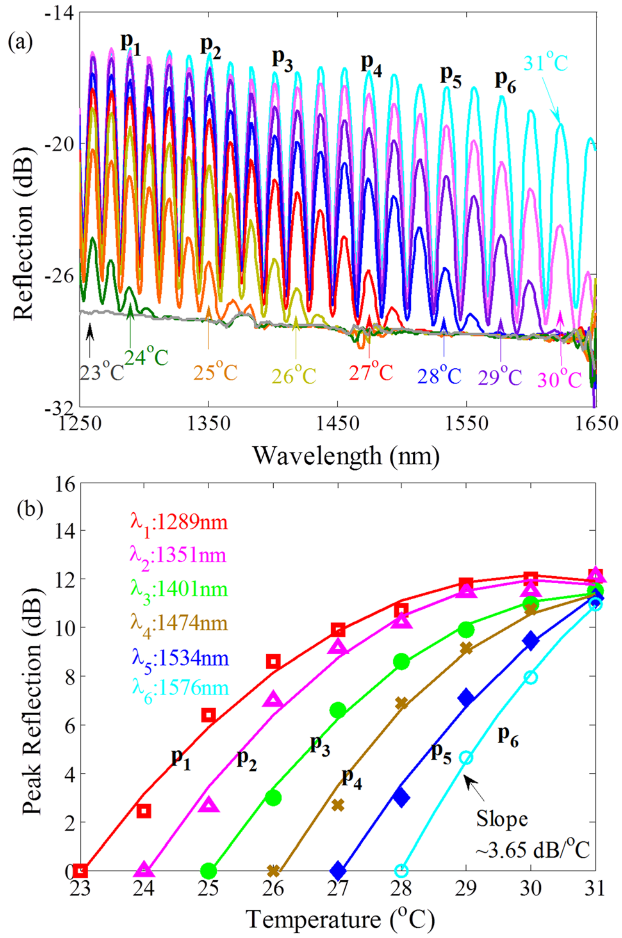

FIG. 5. (a) Reflection spectra of the interference peak with T varies under the FMC condition. (b) T sensitivities of reflection power at different peaks.

almost constant dc-average sinusoidal interference pattern within the wavelength bandwidth of 1250 nm ~ 1650 nm. The experimental result also demonstrates that the interference spectra of the hybrid device with T increases to 1000 °C in the air is not very sensitive with λ shifting but quite linear T sensitivity of 0.0052 nm/°C (~5 pm/°C) obtained, as shown in Fig. 4(b). Inset of the Fig. 4(b) shows the wavelength shift ($\Delta\lambda$) of the monitored spectral fringes. The device has a preferable characteristic for the high *T* sensing application due to the all-silica material configuration. On the other hand, the spectral response of the tapered fiber can be easily modified by applying new optical materials such as optical liquids or other suitable materials surrounding the micro-tapered region. Then, by utilizing this material engineering technique, the waveguide dispersion of the guide mode is changed and the light penetrates out of the silica cladding and reaches into the outer new materials. Thus, to achieve a highly sensitive measurement, a suitable liquid for yielding the FMC condition is used to fill the entire of the hybrid device. As expected, a sinusoidal spectral response is also achieved. The sinusoidal pattern falls along the optical spectral loss at different cutoff λ_c when T varies. However, it still retains the sinusoidal interference pattern in the transition region but peak power changes as T changes, as shown in Fig. 5(a). Figure 5(a) illustrates the development of the optical spectra of the proposed hybrid fiber sensor under FMC condition when T changes from 23 °C to 31 °C. The result shows the sensing capability of monitoring the peak reflection power with good fringe contrast has been achieved by using the hybrid configuration. It also can be clearly seen that the peaks power are greatly varied in the attenuation region. This is because the applied T(°C) controlled by a TE cooler increases to reduce the RI of the surrounding liquid (thermo-optic coefficient $dn/dT = -3.74 \times 10^{-4}\,°C^{-1}$) that makes the cutoff spectra varying greatly to long λ region. Thus, the sensing results can be evaluated by monitoring the peak power of a suitable wavelength fringe since the peak wavelengths (p_i, i = 1, 2…N) are fixed. In the Fig. 5(a), attenuation of the interference peak in the loss region is getting serious when T increases. Therefore the reflection power can be readily measured by a low cost photo-detector at one λ_{pi}, more over a very cheap LED input light may replace the broadband light source those are of the valuable advantages. Fig. 5(b) plots the T sensitivities of many peaks (p_1, p_2,…p_6) marked in the Fig. 5(a). The peak power variations are measured with corresponding to the initial condition of each peak. Experimental results indicate that a very good T response with the peak power varied greatly is performed. Based on the above results, the hybrid fiber-optic device with new optical characteristics has been proposed in the study. Due to the superior sensing ability, we believe that the fiber device can be further integrated into a useful module for high resolution measurement applications.

In conclusion, we have demonstrated a hybrid fiber-optic sensor based on an adiabatic fiber microtaper with an air-gap microcavity fiber Fabry-Pérot interferometer fabricated by a simple fusion splicing method. Interference fringes with high contrast within wide bandwidth of 400 nm are performed by the configuration. The hybrid configuration of the fiber optic sensor can measure the temperature or refractive index or both. Based on the experimental results, a good linearity response for the high T measurement is investigated. Moreover, the sensing capability by monitoring the peak power variation is measured and a high temperature (T) sensitivity of $+3.65\,dB/^{\circ}C$, which is equivalent to RI sensitivity of approximately $+9759\,dB/RIU$ is obtained when the sensor especially operated under the FMC condition.

This research was supported by the National Science Council of the R.O.C., NSC 101-2221-E-239-020 and NSC 102-2221-E-239-033-MY3.

[1]J. D. Love, W. M. Henry, W. J. Stewart, R. J. Black, S. Lacroix, and F. Gonthier, IEE Proc.Optoelectron. **138**(5), 343–354 (1991).
[2]C. L. Lee, Opt. Exp. **18**(14), 14768–14777 (2010).
[3]C. L. Lee, Z. Y. Weng, C. J. Lin, and Y. Y. Lin, Opt. Lett. **35**(24), 4172–4174 (2010).
[4]H. Xuan, W. Jin, and S. Liu, Opt. Lett. **35**(1), 85–87 (2010).
[5]N. Díaz-Herrera, M. C. Navarrete, O. Esteban, and A. González-Cano, Meas. Sci. Technol. **15**(2), 353–358 (2004).
[6]M. Sumetsky, Y. Dulashko, J. M. Fini, and A. Hale, Appl. Phys. Lett. **86**(16), 161108 (2005).
[7]T. A. Birks, W. J. Wadsworth, and St. P. J. Russell, Opt. Lett. **25**(19), 1415–1417(2000).
[8]T. K. Gangopadhyay, Meas. Sci. Technol. **15**, 911–917 (2004).
[9]T. K. Gangopadhyay and P. J. Henderson, Appl. Opt. **38**, 2471–2477 (1999).
[10]C. L. Lee, W. F. Liu, Z. Y. Weng, and F. C. Hu, IEEE Photon. Technol. Lett. **23**(17), 1231–1233(2011).
[11]D. W. Kim, F. Shen, X. Chen, and A. Wang, Opt. Lett. **30**(22), 3000–3002 (2005).
[12]K. Shiraishi, Y. Aizawa, and S. Kawakami, J. Lightwave. Technol. **8**(8), 1151–1161 (1990).
[13]T. K. Gangopadhyay, S. Mandal, K. Dasgupta, T. K. Basak, and S. K. Ghosh, Appl. Opt. **44**(16), 3192–3196 (2005).